



AL-TR-89-085

AD:

Final Report  
for the period  
August 1989 to  
December 1989

# Temperature Measurements Through a Solid-Propellant Combustion Wave Using Imbedded Fine Wire Thermocouples

January 1990

Author:  
D.A. Alspach

AD-A218 642

## Approved for Public Release

Distribution is unlimited. The AL Technical Services Office has reviewed this report, and it is releasable to the National Technical Information Service, where it will be available to the general public, including foreign nationals.

**Astronautics Laboratory (AFSC)**  
Air Force Space Technology Center  
Space Division, Air Force Systems Command  
Edwards Air Force Base, CA 93523-5000

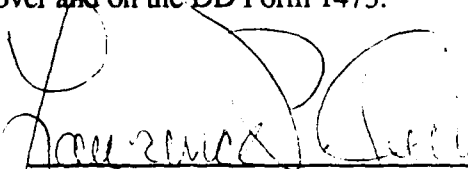


## NOTICE

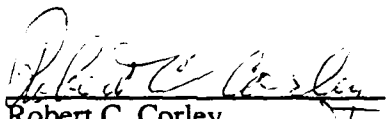
When U.S. Government drawings, specifications, or other data are used for any purpose other than a definitely related Government procurement operation, the fact that the Government may have formulated, furnished, or in any way supplied the said drawings, specifications, or other data, is not to be regarded by implication or otherwise, or in any way licensing the holder or any other person or corporation, or conveying any rights or permission to manufacture, use or sell any patented invention that may be related thereto.

This report has been reviewed and is approved for public release and distribution in accordance with the distribution statement on the cover and on the DD Form 1473.

  
\_\_\_\_\_  
TIM EDWARDS  
Project Manager

  
\_\_\_\_\_  
LAWRENCE P. QUINN  
Chief, Aerothermochemistry Branch

FOR THE DIRECTOR

  
\_\_\_\_\_  
Robert C. Corley  
Director, Astronautical Sciences Division

## REPORT DOCUMENTATION PAGE

Form Approved  
OMB No. 0704-0188

1a. REPORT SECURITY CLASSIFICATION UNCLASSIFIED			1b. RESTRICTIVE MARKINGS		
2a. SECURITY CLASSIFICATION AUTHORITY			3. DISTRIBUTION/AVAILABILITY OF REPORT Approved for Public Release; Distribution is unlimited		
2b. DECLASSIFICATION/DOWNGRADING SCHEDULE					
4. PERFORMING ORGANIZATION REPORT NUMBER(S) AL-TR-89-085			5. MONITORING ORGANIZATION REPORT NUMBER(S)		
6a. NAME OF PERFORMING ORGANIZATION Astronautics Laboratory (AFSC)		6b. OFFICE SYMBOL (If applicable) LSCC		7a. NAME OF MONITORING ORGANIZATION	
6c. ADDRESS (City, State, and ZIP Code) AL/LSCC Edwards AFB CA 93523-5000		7b. ADDRESS (City, State, and ZIP Code)			
8a. NAME OF FUNDING/SPONSORING ORGANIZATION		8b. OFFICE SYMBOL (If applicable)		9. PROCUREMENT INSTRUMENT IDENTIFICATION NUMBER	
8c. ADDRESS (City, State, and ZIP Code)		10. SOURCE OF FUNDING NUMBERS			
		PROGRAM ELEMENT NO. 62302F		PROJECT NO. 5730	TASK NO. 00
				WORK UNIT ACCESSION NO. Q3	
11. TITLE (Include Security Classification) Temperature Measurements Through a Solid-Propellant Combustion Wave Using Imbedded Fine Wire Thermocouples (U)					
12. PERSONAL AUTHOR(S) Alspach, David A.					
13a. TYPE OF REPORT Interim		13b. TIME COVERED FROM 89/08 TO 89/12		14. DATE OF REPORT (Year, Month, Day) 90/01	
				15. PAGE COUNT 25	
16. SUPPLEMENTARY NOTATION					
17. COSATI CODES			18. SUBJECT TERMS (Continue on reverse if necessary and identify by block number)		
FIELD	GROUP	SUB-GROUP			
21	08		Solid propellant combustion, thermocouples		
19. ABSTRACT (Continue on reverse if necessary and identify by block number) Temperature profile measurements have been measured through the combustion wave of burning solid propellant strands using imbedded fine-wire (75-micron diameter) thermocouples. The techniques necessary to construct, imbed, and measure temperature with this size and type of thermocouple were demonstrated. The experiments were performed at pressures ranging from 100 to 450 psi inside a high-pressure test cell designed for this type of operation. Surface temperature measurements have been estimated from the measured profiles for HMX, AN, and Double-Base propellants.					
20. DISTRIBUTION/AVAILABILITY OF ABSTRACT <input checked="" type="checkbox"/> UNCLASSIFIED/UNLIMITED <input type="checkbox"/> SAME AS RPT. <input type="checkbox"/> DTIC USERS			21. ABSTRACT SECURITY CLASSIFICATION UNCLASSIFIED		
22a. NAME OF RESPONSIBLE INDIVIDUAL Tim Edwards			22b. TELEPHONE (Include Area Code) (805) 275-5656		22c. OFFICE SYMBOL AL/LSCC

# TABLE OF CONTENTS

	<u>Page #</u>
Introduction	1
Equipment and Procedures	2
Thermocouple Preparation	2
Strand Preparation	2
Combustor	4
Detectors and Electronics	6
Determination of the Surface Position	7
Determination of Heat Loss Corrections	9
Solid Phase Temperature Measurements	10
Gas Phase Heat Loss Corrections	10
Smoothing of Data	13
Propellant Data	14
Propellant Formulations	14
Propellant Burn Rate Data	14
Temperature Profiles through Combustion Waves	15
HMX2 Propellant Temperature Profiles	16
HMX1 Propellant Temperature Profiles	18
AN Propellant Temperature Profiles	19
Double Base Propellant Temperature Profiles	21
Summary and Conclusions	23
References	24

Accession For	
NTIS GRA&I	<input checked="checked" type="checkbox"/>
DTIC TAB	<input type="checkbox"/>
Unannounced	<input type="checkbox"/>
Justification	
By	
Distribution/	
Availability Codes	
Avail and/or	
Dist	Special
A-1	



## List of Figures

	<u>Page #</u>
Figure 1. Electron microscope photograph of thermocouple constructed from 25 micron wire	3
Figure 2. Thermocouple Welding Bead	3
Figure 3. Horizontal Cut Through Propellant	3
Figure 4. "Sandwich" Construction Technique	3
Figure 5. High Pressure Combustor	5
Figure 6. Thermocouple Feed-Through System	5
Figure 7. Calibration Curve for MacADIOS Board at 100 times gain	6
Figure 8. Mathematical Approximations for Thermocouple Tables	7
Figure 9. Example of Linear Method of Surface Determination	9
Figure 10. Example of Inflection Method of Surface Determination	9
Figure 11. HMX2 Propellant Temperature Profile - 150 psi	16
Figure 12. HMX2 Propellant Temperature Profile - 250 psi	17
Figure 13. HMX2 Propellant Temperature Profile - 450 psi	17
Figure 14. HMX1 Propellant Temperature Profile - 250 psi	18
Figure 15. Demonstration of linear behavior of $\text{Log}(T-T_0)$ vs distance under propellant surface	19
Figure 16. AN Propellant Temperature Profile - 100 psi	20
Figure 17. AN Propellant Temperature Profile - 200 psi	20
Figure 18. AN Propellant Temperature Profile - 300 psi	21
Figure 19. Double Base Temperature Profile - 150 psi	22
Figure 20. Double Base Temperature Profile - 250 psi	22

## List of Tables

Table 1. Propellant Formulations	14
Table 2. Propellant Burn Rate Data	14
Table 3. Summary of Results	15
Table 4. Comparison of Data	16

## Introduction

The purpose of this technical report is to document the experimental results obtained during the author's Co-Op work session from 28 August 1989 through 15 December 1989. The author is a junior at Purdue University, West Lafayette, IN and was employed in the Combustion Research Laboratory of the Air Force Astronautics Laboratory (AFSC), Edwards Air Force Base, CA. All experimentation was conducted at this facility. The experiment involved the measurement of temperature profiles through the combustion wave of solid propellants using fine thermocouples. This experiment was part of a larger study into solid propellant combustion mechanisms. The temperature profiles being measured are a valuable tool in the analysis and modeling of solid propellant combustion chemistry. Temperature profiles were measured for four different types of solid propellant: AN/energetic binder, HMX/energetic binder, HMX/inert binder, and double-base.

## Equipment and Procedures

### Thermocouple Preparation

The thermocouples used in this experiment were Standard Type-S (Platinum vs. Platinum-10% Rhodium) and Type-R (Platinum vs. Platinum-13% Rhodium). These types of thermocouples were chosen due to their relatively high melting point (a sustained 1800 K) and their inherent chemical stability. Two different wire diameters, 75-micron and 25-micron, were used. The 75-micron wire was used to give a general picture of the temperature profile in the combustion wave while the 25-micron was used when a more detailed analysis using finer spatial resolution was required. All profiles presented in this report were measured using the relatively large 75-micron diameter thermocouples.

Although factory prepared thermocouples of this size are available, the thermocouples were constructed in-house to develop the techniques necessary to construct thermocouples smaller than those readily available. In this way, when the experiment reaches the point where extremely small thermocouples are required, the groundwork will have already been established. In-house construction also allowed for the close monitoring of weld quality and bead size.

A junction welding technique, using either a butane-oxygen or a propane-oxygen torch system, was developed to construct the fine-wire thermocouples. This technique involved holding the thermocouple wires between two magnets and positioning them so that their tips were crossing. The torch was adjusted so that a neutral flame no longer than 7.5 mm was achieved. The torch was brought up to the crossed-tips to a position where the thermocouple wire started to melt. As each wire melted, it produced a small bead of metal which receded up the wire as heating was continued. When the two beads came together and mixed, the torch was quickly removed and the junction was complete. The bead was inspected under a 30 power microscope to measure bead size and check for weld quality. The bead size was limited to three times the wire diameter to insure consistent response times. The continuity of the thermocouple was checked by using a Fluke multimeter set to measure resistance. A successful thermocouple was determined by comparing the resistance measured to the standard values.<sup>1</sup> An example of a properly constructed thermocouple is shown in Figures 1 and 2. Now that this technique has been proven successful, construction of even smaller thermocouples, perhaps ten or more times, is possible.

### Strand Preparation

The propellant was prepared in strands of about 3-4 cm in length and approximately 6 mm in diameter. The technique used for imbedding the fine thermocouples greatly depends upon the type of propellant in question. For the propellants used in this experiment, two different techniques were employed.

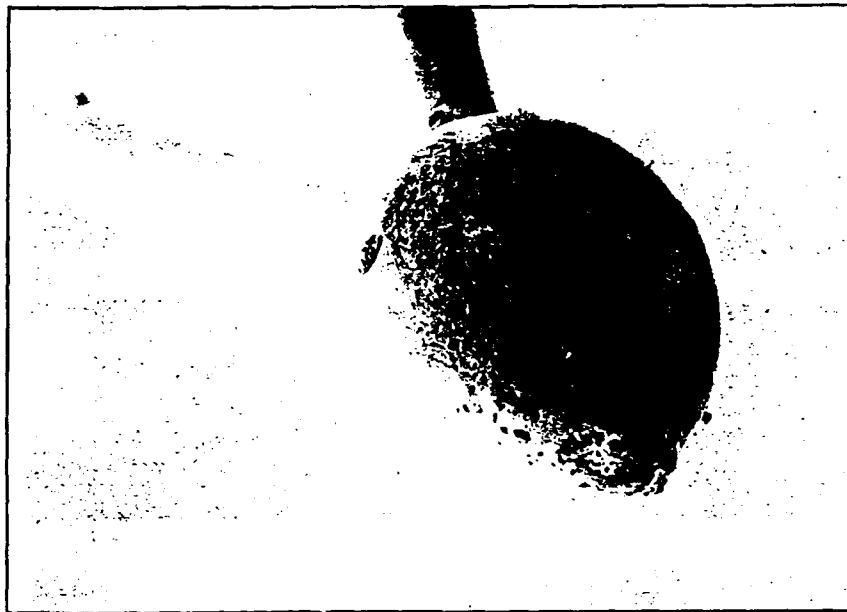


Figure 1. Electron microscope photograph of thermocouple constructed from 25 micron wire. (Note: Exaggerated bead size due to perspective. Actual bead size approx. 50-75 micron.)

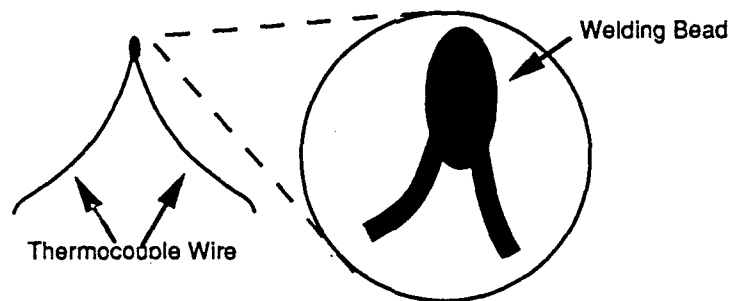


Figure 2. Thermocouple Welding Bead

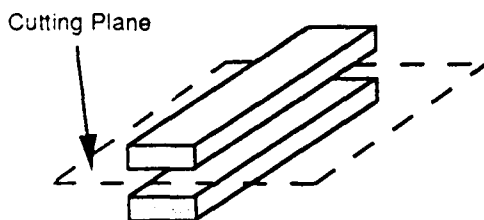


Figure 3. Horizontal Cut Through Propellant

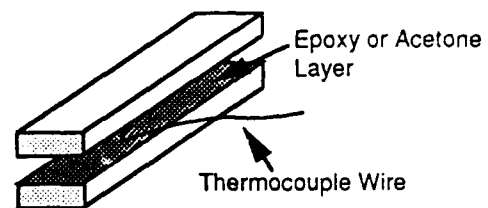


Figure 4. "Sandwich" Construction Technique



Both methods use a sandwich construction technique. Construction began by making a flat, horizontal cut lengthwise through the propellant strands using a razor blade (Fig. 3). The two halves were separated with the cutting plane facing upwards. The thermocouple was placed onto one of the sections. A layer of binder which would hold the two sections back together was next applied.

The first method for binding the two halves of the strand together was a technique described by Kubota, et al.<sup>2</sup> This technique uses acetone to dissolve the propellant's own binder, forming a "glue-like" liquid layer which is used to bind the two sections back together. The acetone was spread over the whole surface using a brush. The second section was then placed on top of the first to form a sandwich with the thermocouple (Fig. 4). The two sections were compressed using a vise to insure a uniform surface between the two sections. The strands were then left to dry, typically for three days. This method was successful only for the double-base propellants. The binders of the other propellants were apparently not sufficiently soluble in acetone for successful use of this binding method. The binding layer used in the HMX or AN propellants was an epoxy adhesive (Devcon 5-minute Epoxy). The epoxy serves as a strong binder to join the two section back together. The surface was coated with a fine layer of epoxy using a knife and the thermocouple pressed into the layer so that its bead was pressed into the propellant. The strands were then left to dry overnight. After the propellant strands prepared by either method were dry, the thermocouples were again tested for continuity using a Fluke multimeter set to measure resistance.

The author admits that there is still some uncertainty about the epoxy's effect on the thermocouple measurement. Initial burn rate and temperature measurement experiments do not indicate noticeable differences with expected or previously collected data<sup>3</sup>, but a more complete study is needed. Future research should investigate the effects, if any, of this binding technique.

To complete the strand preparation process, the sides of the strands were coated with a thin layer of fluorocarbon grease which acted as a burn inhibitor. This was done to insure a flat burning surface during tests.

## **Combustor**

The experiments were carried out inside a nitrogen-purged, high pressure combustor<sup>4</sup> designed for strand burning of this type. The chamber is capable of pressures ranging from atmospheric to 1000 psig. The imbedded thermocouples were attached to a thermocouple compensated modular coupling junction and the signal was passed through a Conax HMC Compression Fitting using thermocouple compensated extension wire to the data-acquisition computer outside. The combustor and feed-through system are illustrated in Figures 5 and 6.

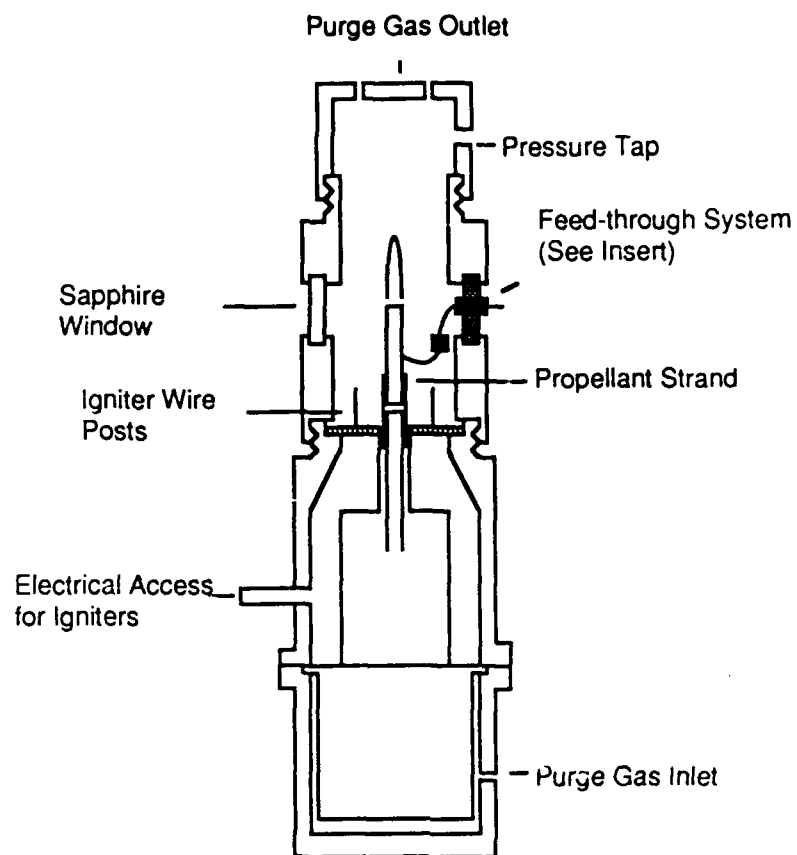


Figure 5. High Pressure Combustor

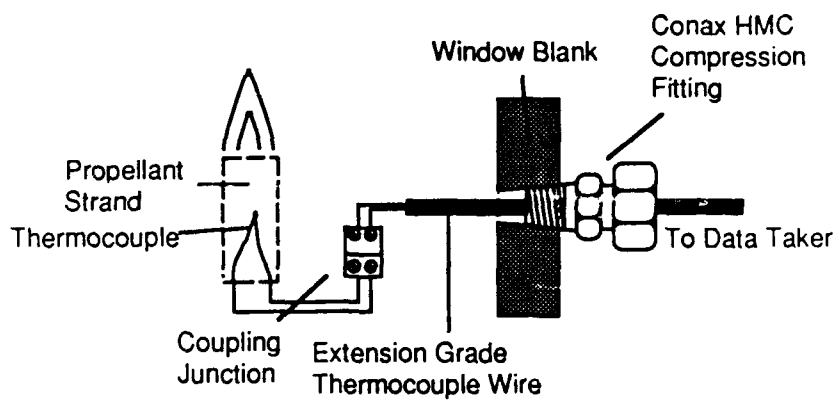


Figure 6. Thermocouple Feed-Through System

## Detectors and Electronics

The raw analog voltage signal collection from the thermocouples was handled by an Apple Macintosh IIx through a MacADIOS A/D board. The software used to collect and simultaneously graph the data was written for another in-house experiment.<sup>5</sup> The data collection system takes data asynchronously at a rate which was determined to be approximately 200 Hz. There is an associated error in this measurement of approximately  $\pm 10\%$ . Post processing for signal conditioning and heat loss effects was done on an Apple Macintosh SE using another in-house software package.<sup>6</sup>

The signal conditioning package takes the raw data from the computer and converts it from the arbitrary units put out by the A/D board into millivolts. The correction factor was determined by inputting into the data collection system a known wave (in this case a sine-wave) using a function generator. By taking the known amplitude at several points and comparing these to the numbers put out by the A/D board, a calibration curve could be drawn (Fig. 7).

The signal conditioner then converts the millivolts into temperature using a curve fit to the National Bureau of Standards Thermocouple Tables (Fig. 8). This program also calculates relative times and distances from the first point using sampling and burn rate data. This raw data set was used in the determination of the position of the burning surface, as described below.

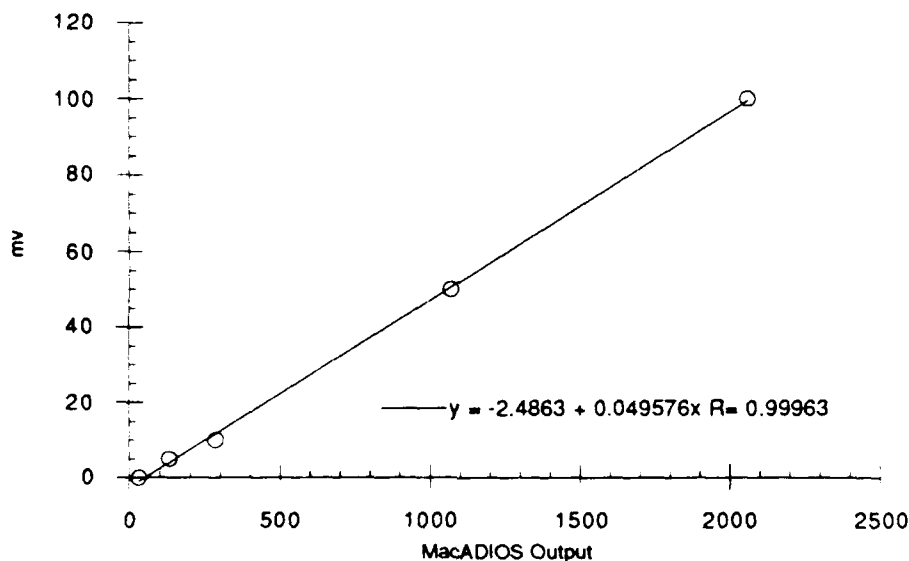


Figure 7. Calibration Curve for MacADIOS Board at 100 times gain.

Conversion for Type-R and Type-S Thermocouple Readings  
Curve fit to National Bureau of Standards Thermocouple Tables

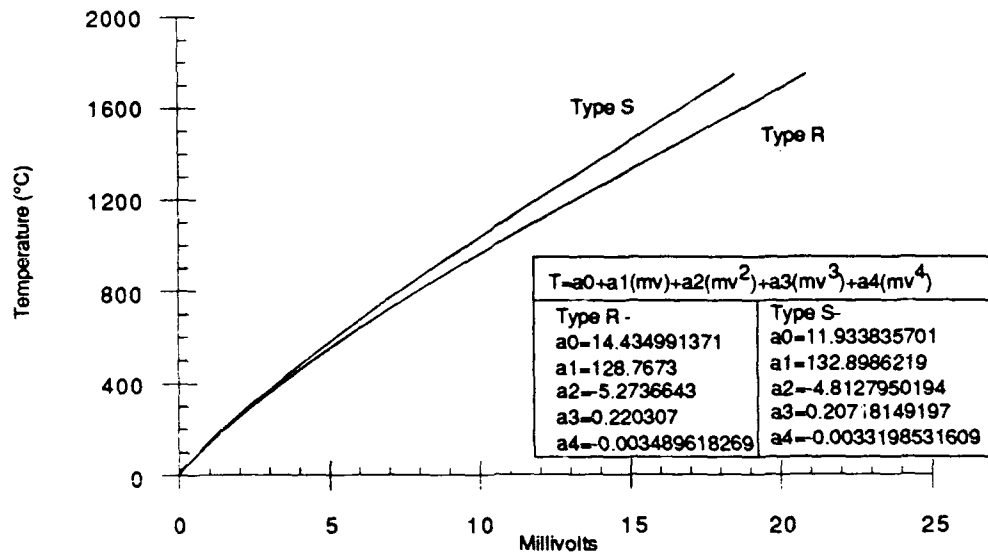


Figure 8. Mathematical Approximations for Thermocouple Tables.

### Determination of Surface Position

The technique used to determine the position of the burning surface of the propellant was similar to that described by Sabadell, et al.<sup>7</sup> They describe the one-dimensional flow of heat in a medium with heat generation  $\dot{q}_x$  as:

$$\frac{\delta}{\delta x} \left( -\lambda \frac{\delta T}{\delta x} + \dot{m} C_p (T - T_0) \right) = \dot{q}_x \quad (1)$$

where;

$\dot{m}$  = mass flow rate of propellant

$C_p$  = specific heat

$\lambda$  = thermal conductivity

$\dot{q}_x$  = rate of heat generation

If the specific heat,  $C_p$ , and the thermal conductivity,  $\lambda$ , are assumed to be constant over the range of integration, the heat flow formula can be integrated to give:

$$\frac{d \ln(T - T_0)}{dx} = \frac{\dot{m} C_p}{\lambda} - \frac{1}{(T - T_0) \lambda} \int \dot{q}_x dx \quad (2)$$

According to a model proposed by Kubota,<sup>8</sup> the chemical reactions in the solid phase are negligibly small, therefore the heat generation from the chemical reaction is virtually zero. If we let  $\dot{q}_x$  approach zero, the above equation becomes:

$$\frac{d \ln(T-T_0)}{dx} = \frac{mC_p}{\lambda} \quad (3)$$

Inside the solid propellant where this assumption holds true ( $\dot{q}_x \rightarrow 0$ ), the graph of  $\ln(T-T_0)$  against  $x$  would be a straight line. But as soon as these assumptions break down, e.g., heat is produced by chemical reactions, this graph against  $x$  would no longer be linear. This deviation could represent the passing of the thermocouple from the solid phase through the surface of the burning propellant into the gas phase. Therefore, in the regions where the curve was linear, the thermocouple tip was assumed to be inside the propellant. The point where the curve changed from linear to nonlinear was assumed to be the burning surface position, and all points after that were assumed to be in the gas phase. An example of this technique is shown in Figure 9.

The surface position is also detectable on a graph of temperature versus distance  $x$ , although much less obvious (Fig. 10). The curve has an inflection point from concave upward to concave downward at or near the point where the thermocouple passes through the surface. The change is also due to the different mechanisms of heat transfer in the solid and gas phases.

There is a degree of error associated in determining the surface positions using any technique due to human interpretation, limits of accuracy, etc. For a typical temperature profile, the uncertainty in determining the surface position may be as high as  $\pm 50$  K. This uncertainty due to these effects should be taken into account when interpreting the surface temperatures presented in this report.

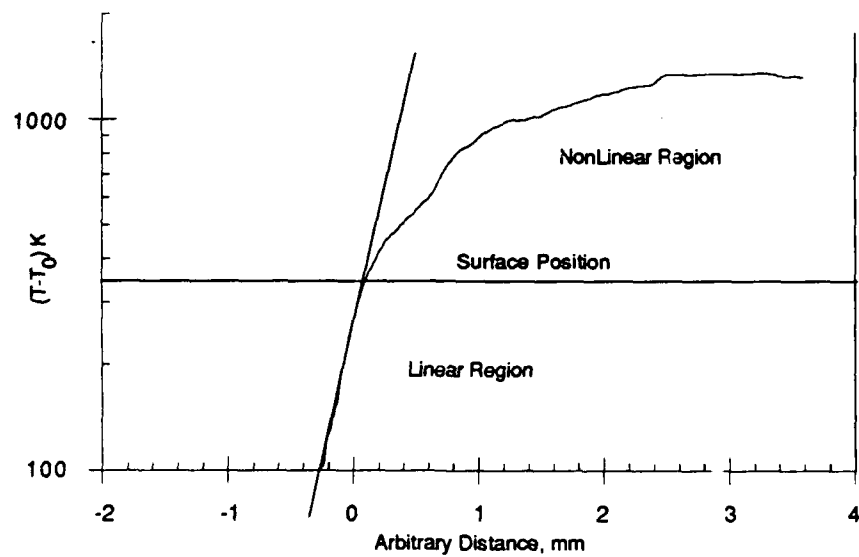


Figure 9. Example of Linear Method of Surface Determination.

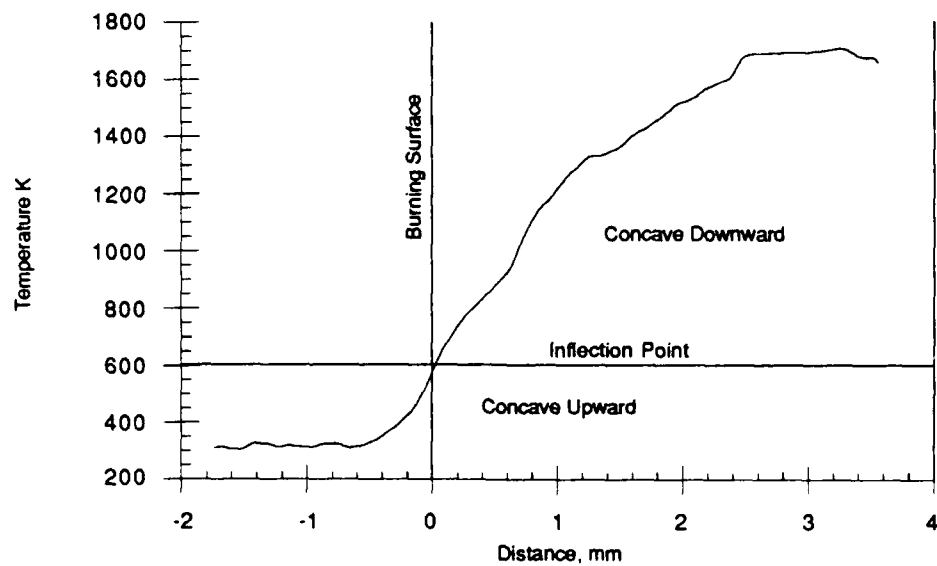


Figure 10. Example of Inflection Method of Surface Determination.

## Determination of Heat Loss Corrections

The measurements taken by the thermocouple represent merely the temperature of the tip of the thermocouple, and may not truly represent the temperature of the surrounding medium. There are various effects, such as radiation and conduction of heat, which may cause this difference. To show a true representation of the actual medium temperature, these effects must be taken into account.

**Solid Phase Temperature Measurements.** The thermocouple temperature measurements, in the solid phase, measure the temperature of the solid propellant as it is slowly heated from above. The temperature measurements must be corrected for heat loss effects. Loss due to radiation is not possible in the solid phase because the thermocouple is entirely imbedded in the solid propellant. The only type of loss possible is conduction of heat down the thermocouple wires. A simplified model was used to perform an order of magnitude calculation for the conductive heat loss. The thermocouple tip was assumed to be at a temperature  $T_t$  while the heat sink inside the solid propellant was at  $T_s$ , which was at an arbitrary but finite distance  $x_1$  away. Therefore, there will be an interchange of convective heat energy between these two regions which can be described by Fourier's law:

$$\dot{Q}_{cd} = -kA \frac{dT}{dx} \quad (4)$$

where;

$\dot{Q}_{cd}$  = rate of heat flow, W

$k$  = thermal conductivity of the material, W/(K m)

$A$  = Area perpendicular to heat flow  $m^2$

$dT/dx$  = temperature gradient in direction of heat flow, K/m

In this particular example, using a Type-S thermocouple with a wire diameter of 75-microns, the equation becomes:

$k = 71.8 \text{ W/m K}$  (See Footnote<sup>9</sup>)

$A_{total} = 9.1207 \times 10^{-9} \text{ m}^2$

$$\dot{Q}_{cd} = -(6.5487 \times 10^{-7}) \frac{T_t - T_s}{x_1} \quad (5)$$

It can be seen from this equation that if the quantity  $(T_t - T_s)$  remains relatively small (say < 700), and  $x_1$  is finite, then the heat loss due to conduction is negligibly small. Therefore in this experiment, no corrections for heat loss were made in the solid phase.

**Gas Phase Heat Loss Corrections.** In the gas phase, the tip of the thermocouple has protruded through the burning surface and is measuring the temperature of the gases evolving off of the burning surface of the propellant. There are losses associated with this region as well. As before, the thermocouple can conduct heat down the wires, but because

it is now exposed to flowing gases, the thermocouple can also radiated heat outwards to the combustor walls, and can be convectively heated by the flowing gas.

The correction for loss due to conduction in the gas phase was treated in much the same way as in the solid phase. The thermocouple tip was again assumed to be at  $T_t$ , and the heat sink was assumed to be inside the propellant at  $T_s$  an arbitrary but finite distance  $x_1$  away. It was previously shown that the heat loss due to conduction in such a case with a typical thermocouple (Type-S, 75-micron diameter wire) is:

$$\dot{Q}_{cd} = -(6.5487 \times 10^{-7}) \frac{T_t - T_s}{x_1} \quad (6)$$

Unlike the solid phase the quantity  $(T_t - T_s)$  can no longer be assumed to be relatively small considering flame temperatures above 2000 K. Thus, the effects due to conduction in the gas phase cannot be neglected.

In the gas phase, the thermocouple may also radiate heat to a sink, in this case the combustor walls. The model used to calculate the loss due to radiation was as follows. The thermocouple bead and combustor were modeled as concentric spheres with surface areas  $A_t$  and  $A_c$  respectively. The thermocouple tip was assumed to be at  $T_t$  while the combustor was at  $T_c$ , which is assumed to be a heat sink and remain at room temperature. Therefore, there will be an interchange of radiant energy between these two regions which is described by the Stefan-Boltzmann radiation equation for two concentric spheres:

$$\dot{Q}_r = \left( \frac{C_b}{\frac{1}{\epsilon_t} + \frac{A_t}{A_c} \left( \frac{1}{\epsilon_c} - 1 \right)} \right) A_t (T_t^4 - T_c^4) \quad (7)$$

where;

$\dot{Q}_r$  = emitted energy, W

$C_b$  = radiation coefficient for a black body

$A_t$  = Surface area of the thermocouple bead,  $m^2$

$A_c$  = Surface area of the inside of combustor,  $m^2$

$T_t$  = Surface temperature of the thermocouple bead, K

$T_c$  = Surface temperature of the combustor, K

$\epsilon_t$  = emissivity of thermocouple material

$\epsilon_c$  = emissivity of inside of combustor

Again for the typical thermocouple (Type-S, bead diameter  $\approx$  225-microns), and the combustor used in this experiment (inner diameter  $\approx$  10 cm), the heat loss due to radiation can be written as:



$$\begin{aligned}
C_b &= 5.7 \times 10^{-8} \text{ W/m}^2\text{K}^4 & (\text{Reference 10}) \\
A_t &= 2.2027 \times 10^{-7} \text{ m}^2 \\
A_c &= 3.243 \times 10^{-2} \text{ m}^2 \\
\epsilon_t &= 0.03 \text{ and } \epsilon_c = 0.7 & (\text{Reference 10})
\end{aligned}$$

$$\dot{Q}_r = (3.7666 \times 10^{-16})(T_t^4 - T_c^4) \quad (8)$$

This heat loss effect cannot be neglected because the quantity  $(T_t^4 - T_c^4)$  cannot be assumed to be small. Therefore, the total heat lost by the thermocouple tip in the gas phase is:

$$\dot{Q}_{\text{total loss}} = \dot{Q}_{cd} + \dot{Q}_r \quad (9)$$

Plugging in the known values, this becomes:

$$\dot{Q}_{\text{total loss}} = (-6.5487 \times 10^{-7})\left(\frac{T_r - T_s}{x_1}\right) - (3.7666 \times 10^{-16})(T_t^4 - T_c^4) \quad (10)$$

If the thermocouple tip is assumed to be in a quasi-steady-state where the temperature is constant over a short time interval, the total heat lost by the thermocouple tip is balanced by the heat gained by convective heating.

The thermocouple tip at  $T_t$  is convectively heated by the hot gases evolving off the burning surface at  $T_g$ . The heat gained by convection must equal the total heat lost and is given by the following system of equations:

$$\dot{Q}_{\text{convection}} = \bar{h}A(T_t - T_g) \quad (11)$$

where;  $\dot{Q}_{\text{convection}}$  = heat gained by convection  
 $\bar{h}$  = convective heat transfer coefficient

$$\bar{h} = \frac{\overline{Nu_D} k}{D} \quad (12)$$

where;  $\overline{Nu_D}$  = Nusselt number for gas at  $T_g$   
 $k$  = thermal conductivity of thermocouple metal  
 $D$  = thermocouple bead diameter

$$\overline{Nu_D} = 2 + (0.4Re_D^{0.5} + 0.06Re_D^{0.667})(Pr^{0.4})\left(\frac{\mu}{\mu_s}\right)^{0.25} \quad (13)$$

where;  
 $Re_D$  = Reynolds number for thermocouple bead in gas at  $T_g$   
 $Pr$  = Prandtl's number for gas at  $T_g$   
 $\mu$  = dynamic viscosity for gas at  $T_g$   
 $\mu_s$  = dynamic viscosity for gas at  $T_t$

$$Re_D = \frac{vD}{\gamma} \quad (14)$$

where;  
 $v$  = velocity of evolving gas  
 $D$  = thermocouple bead diameter  
 $\nu$  = kinematic viscosity of gas at  $T_g$

$$\gamma = \left( \frac{\rho_{\text{propellant}}}{\rho_{\text{gas}}} \right) (\text{burn rate}) \quad (15)$$

where;  
 $\rho_{\text{propellant}}$  = density of solid propellant  
 $\rho_{\text{gas}}$  = density of evolving gas

To solve for the actual temperature of the gas,  $T_g$ , all the gas properties<sup>11</sup> were first taken at  $T_t$ . The above equations were solved and an intermediate gas temperature was found. The gas properties were then found at the intermediate temperature and the equations were solved again. This iteration continued until the gas temperature  $T_g$  settled to a given value. This temperature is then assumed to be the actual gas temperature.

In general, the effects due to heat transfer were small when compared to the overall temperature and the imprecision of gas phase temperature measurements under these conditions. A typical corrected temperature was at a maximum approximately 4% higher than the measured temperature, which is well below other expected sources of experimental error in measurements of this type. The maximum correction was generally consistent regardless of propellant type, pressure, or temperature.

### Smoothing of Data

All data for the temperature profiles presented in this report have been smoothed to remove noise. The noise in the signal is believed to be background from the A/D board. The amount of noise present was consistent in magnitude regardless of the level of input signal. The noise was also present when a function generator was used to deliver a steady signal to the input device. From these two facts, it was concluded that the noise was not true signal detail and the data would not be adversely affected by removing it.

## Propellant Data

### Propellant Formulations

Most of the propellants used in this experiments were produced at the Astronautics Lab. Their formulations<sup>12</sup> are given below.

Table 1. Propellant Formulations

	HMX2	HMX1	AN	DB1
Ingredient, wt % (approx)				
HMX (200/20 $\mu$ m)	80	73	0	0
PGA binder	20	10	0	0
PEG binder	0	0	0	29
TMETN	0	17	12	0
NG	0	0	0	71
AN	0	0	67	0
GAP binder	0	0	21	0

HMX = cyclotetramethylene tetranitramine  $C_4H_8N_8O_8$

NG = nitroglycerin  $C_3H_5N_3O_9$

PGA = polydiethylene glycol adipate  $C_{4.58}H_{7.50}O_{2.34}$

AN = ammonium nitrate  $NH_4NO_3$

PEG = polyethylene glycol-based polymer  $C_{4.5}H_{9.1}O_{2.3}$

GAP = glycidyl azide polymer

TMETN = trimethyloethanetrinitrate  $C_5H_9O_9N_3$

### Propellant Burn Rate Data

Table 2. Propellant Burn Rate Data

Pressure (psi)	HMX2	HMX1	AN	DB1
100	no burn	.842	1.496	2.693
150	.650	1.057	2.075	2.893
200	.750	1.272	2.653	3.094
250	1.000	1.488	3.231	3.295
300	1.200	1.703	3.809	3.495
450	1.400	2.348	5.544	4.097

HMX2 Data from Kubota, N., *Physicochemical Processes of HMX Propellant Combustion*, 19th Symposium on Combustion, p. 779 (1982).

Other Data from Edwards, J.T., *Solid Propellant Flame Spectroscopy*, AFAL-TR-88-076, Air Force Propulsion Lab, Edwards AFB, CA, August 1988.

## Temperature Profiles through Combustion Waves

The results from this experiment are presented below. In the short time available, trials were performed for four different propellants (HMX2, HMX1, AN, and double base). This was done to aid in future research projects concentrating on specific propellants at the lab. No attempt is made in this report to interpret the results, this will be left to future research. A summary of important temperatures is presented in Table 3.

Table 3. Summary of Results

Propellant	Pressure	No. of Runs	T <sub>s</sub> (K)	T <sub>max</sub> (K)
HMX2	150	1	700	1050
	250	3	700	1500
	450	4	700	>2000
HMX1	250	1	750	>2000
AN	100	4	600	1200
	200	2	600	1800
	300	2	600	1800
Double Base	150	1	575	1300
	250	1	550	1500

T<sub>max</sub> should not be interpreted as the maximum adiabatic equilibrium flame temperature. This is the maximum observed temperature during the experimental burn but does not necessarily represent the maximum flame temperature. This reading can be expected to be low for variety of reasons, the most significant one is that the thermocouples may not read throughout the entire flame structure. Thermocouples of this size are extremely fragile, which often results in them being blown to the side by the fast flowing gases evolving off the propellant surface.

Also, temperature measurements given as a lower limit are listed that way because the thermocouple was destroyed while the temperature was at or near that level and rising.

Due to space and time requirements, not all performed trials are shown in detail. Only one representative trial for each propellant at each pressure is presented. All the temperature profiles presented in this report were taken with 75-micron thermocouples. Although some temperature profiles were measured using 25-micron thermocouples, they are not presented in this report. This was done to present consistent results without having to consider the possible effects of the smaller thermocouples. When available, data from multiple trials was compared to check for reproducibility. Thus, it should be taken into account that although there is no obvious reproducibility problem within other data sets, there is no evidence of reproducibility at the present time for propellants and pressures with only one trial.

## HMX2 Propellant Temperature Profiles

The first data set obtained was for the HMX2 propellant. These trials were done for calibration and testing purposes. Temperature profiles were available for HMX2 from Kubota<sup>3</sup> and others, so the goal for the first set was to reproduce this data. Temperature profiles were taken for HMX2 at three different pressures: 150, 250, and 450 psi. These pressures were chosen to ease the comparison between data sets. Figures 11-13 show the temperature profiles for the three pressures. The data agrees reasonably well with Kubota's data for this single propellant and therefore establishes the accuracy of this method. A brief comparison between the two data sets is shown in Table 4.

Table 4. Comparison of Data

Pressure	Alspach		Kubota	
	Surface Temp(K)	Maximum Temp(K)	Surface Temp(K)	Maximum Temp(K)
≈150 psi	700	1050	673	975
≈450 psi	700	1900	673	1873

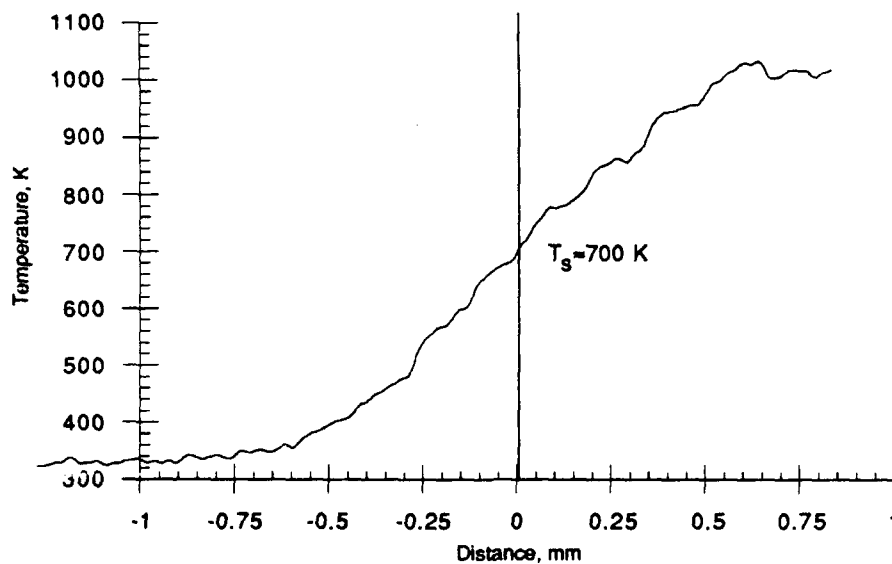


Figure 11. HMX2 Propellant Temperature Profile - 150 psi.

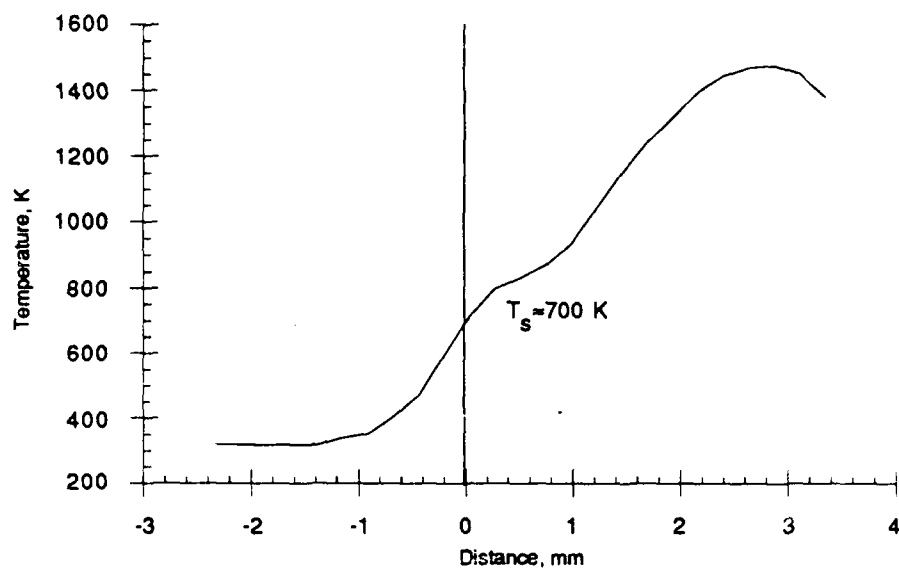


Figure 12. HMX2 Propellant Temperature Profile - 250 psi.

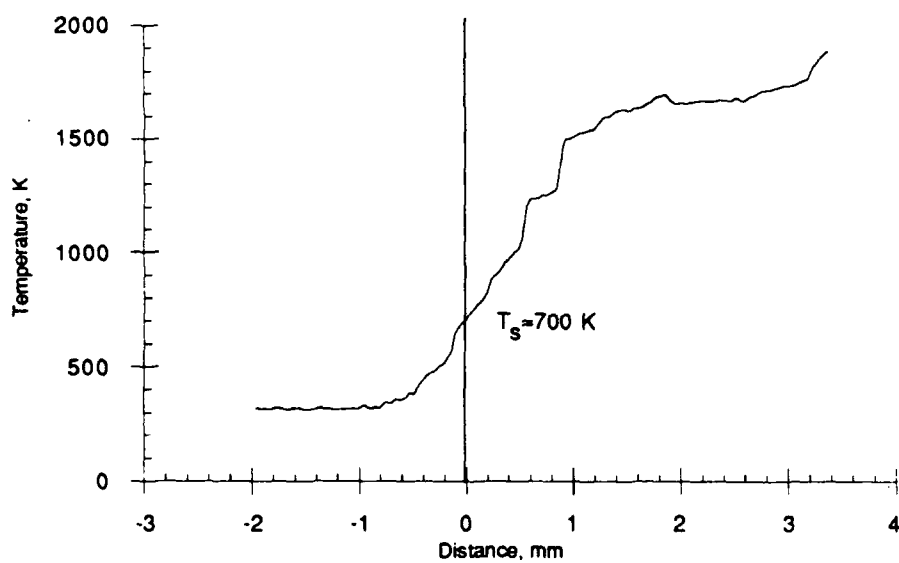


Figure 13. HMX2 Propellant Temperature Profile - 450 psi.

## HMX1 Propellant Temperature Profiles

A different mix of HMX was tried to examine higher temperature readings. The propellant called HMX1 is known to burn at a much higher temperatures than HMX2, therefore it was chosen for the high temperature tests. Only one trial at 250 psi was attempted for this propellant. The temperature profile is presented in Figure 14. This is an interesting profile because it demonstrated the unusual behavior of thermocouples above the recommended operating range. Notice the unusual behavior beginning at approximately 1500 K and the rapid leveling off at 1900 K. The endpoint of this profile is the location of the onset of random fluctuations in the signal. This sequence beginning at 1500 K could represent the thermocouple's response to extremely rapid heating, the onset of the bead melting, and the destruction of the thermocouple.

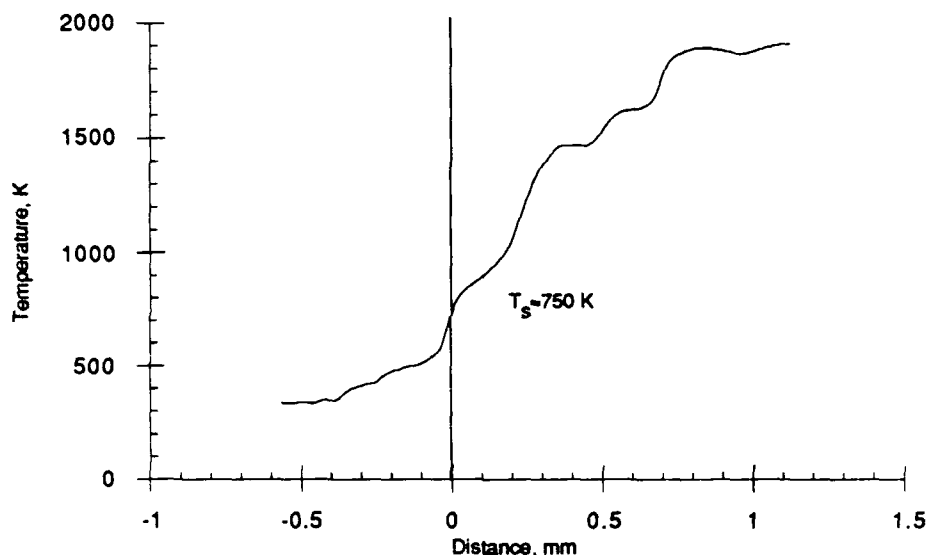


Figure 14. HMX1 Propellant Temperature Profile - 250 psi.

## AN Propellant Temperature Profiles

By far the most significant temperature profiles obtained in this experiment are those for the AN based propellant. There has been little modeling conducted for AN propellants in the past. But studies of AN propellants have gained momentum recently because of a renewed interest in AN's potential use as a "clean" fuel which would not produce any HCl. AN propellant was studied at three different pressures: 100, 200, and 300 psi. The surface temperature for all three pressures was approximately the same,  $600 \pm 25$  K ( $T-T_0 \approx 325 \pm 25$  K). This is in line with experiments currently being done by other researchers.<sup>13</sup> Figure 15 shows the consistent surface temperature minus ambient temperature readings for the three pressures, and is a good example of the linear method used in determining surface position. Figures 16-18 show the temperature profiles for the three different pressures.

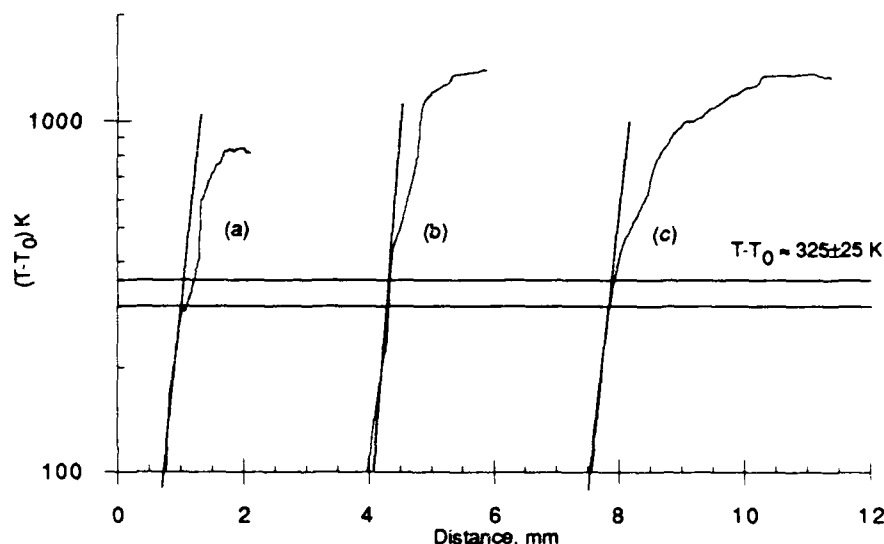


Figure 15. Demonstration of linear behavior of  $\log(T-T_0) K$  vs distance under propellant surface. a) AN Propellant - 100 psi, b) AN Propellant - 200 psi, and c) AN Propellant - 300 psi.



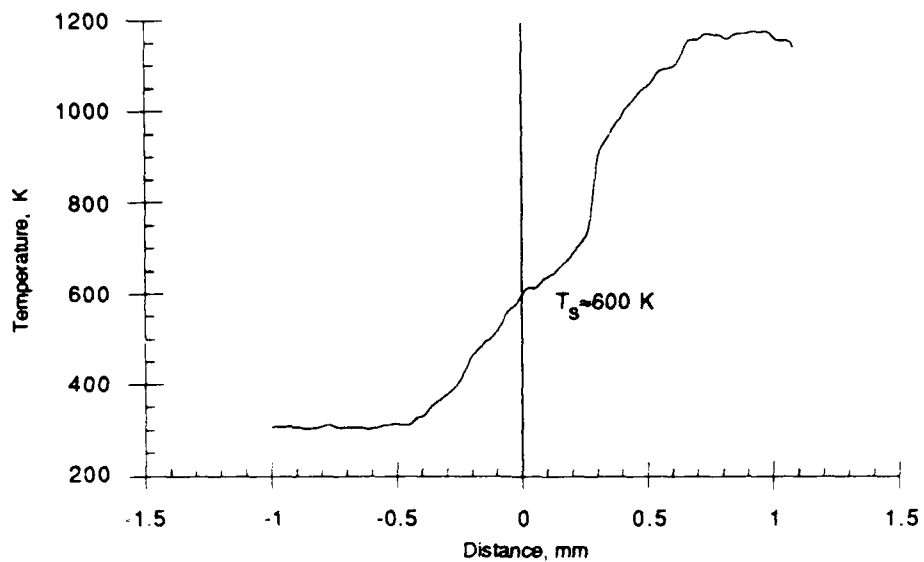


Figure 16. AN Propellant Temperature Profile - 100 psi.

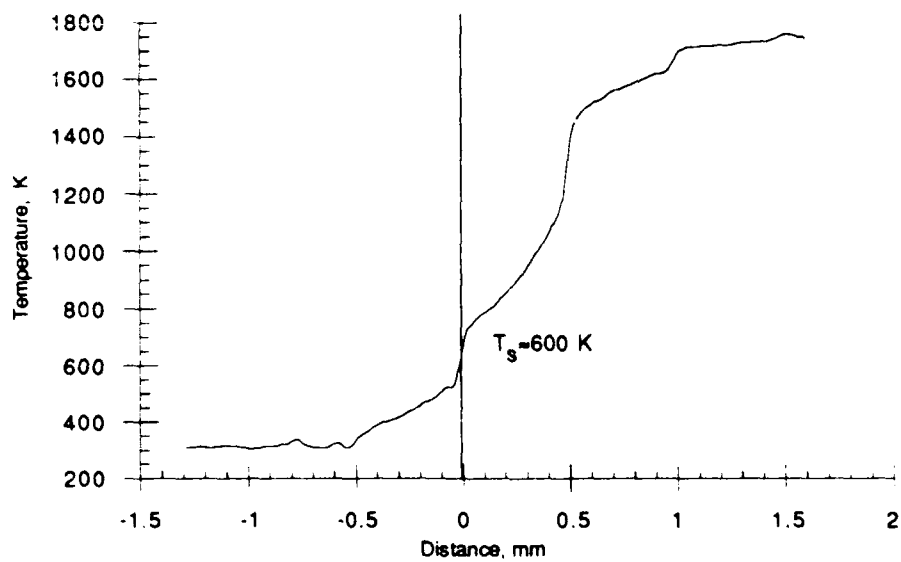


Figure 17. AN Propellant Temperature Profile - 200 psi.

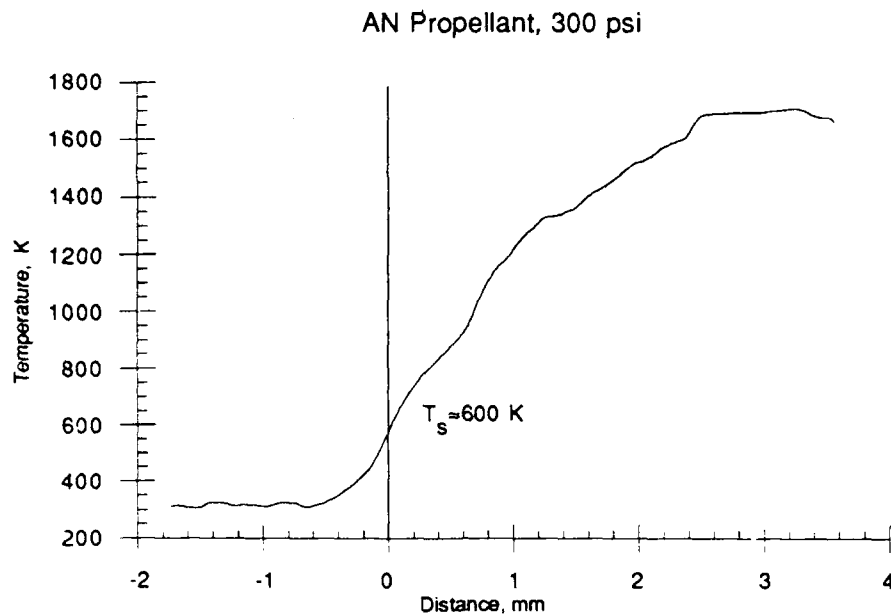


Figure 18. AN Propellant Temperature Profile - 300 psi.

### Double Base Propellant Temperature Profiles

Some double base propellant experiments were performed to add to the variety of propellants tested. This enabled techniques to be developed for propellants which have a more rubberized binder and can take advantage of the acetone binding technique. Data sets for double-base propellants were also available from other research<sup>7</sup> and served as a second set of data for comparison purposes. The data from this experiment also matched the comparison set reasonably well. Trials were performed for the double-base propellants at two different pressures: 150, and 250 psi. The temperature profiles are shown in Figures 19-20.

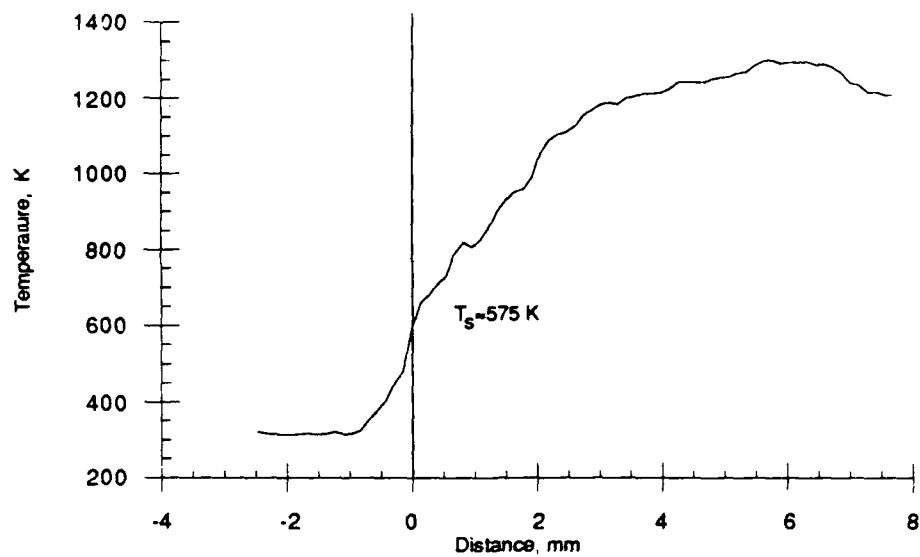


Figure 19. Double Base Propellant Temperature Profile - 150 psi.

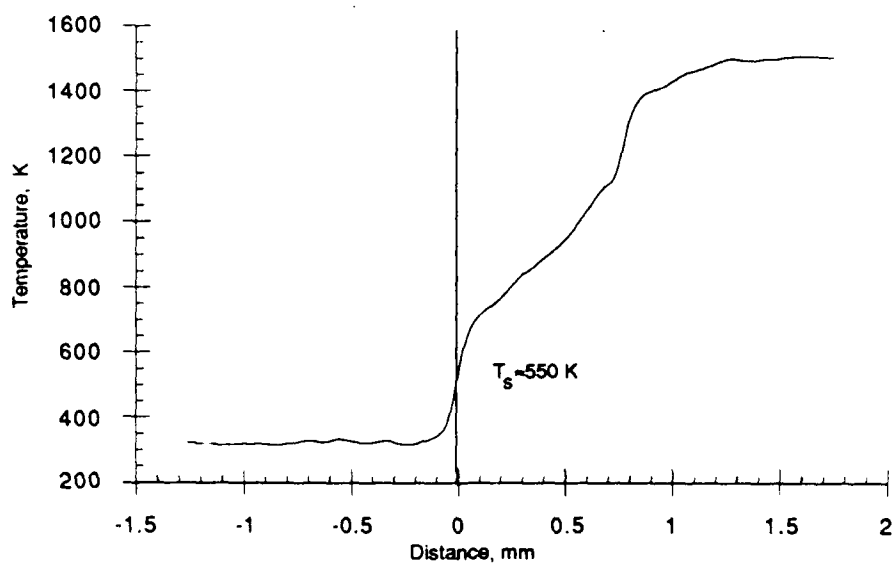


Figure 20. Double Base Propellant Temperature Profile - 250 psi.

## Summary and Conclusions

While this report presents only a limited amount of data and makes no attempt to analyze it, the ability now exists to measure temperature profiles for any number of solid propellants using a range of thermocouple sizes. Now that the technique has been developed at the Astronautics Laboratory, it will hopefully be exploited in further studies concentrating on specific propellants. While this report does not answer all the questions concerning the use of fine thermocouples in this manner, future research should be able to build upon the groundwork set down at the laboratory during this short time period; such as construction technique, data acquisition, etc., and should further broaden the understanding of the thermocouple technique.

## References

1. Thermocouple Wire Size and Resistance Table, *National Bureau of Standards Thermocouple Tables*, Omega Catalog, Table K, p. T-38. Vol. 26, [1988].
2. Kubota, N., "The Mechanism of Super-Rate Burning of Catalyzed Double Base Propellants", *Princeton Technical Report AMSR 1087 (Kubota's PhD thesis)*, Princeton University, pp. C7-C8 (1973).
3. Kubota, N., "Physicochemical Processes of HMX Propellant Combustion", *Nineteenth Symposium on Combustion*, pp. 777-785 (1982).
4. Edwards, T., Weaver, D.P., Campbell, D.H., and Hulsizer, S., "A High Pressure Combustor for the Spectroscopic Study of Solid Propellant Combustion Chemistry," *Review of Scientific Instruments*, Vol. 56, No. 11, pp. 2131-2137, 1985.
5. Zabarnick, S., *MacADIOS.SZ*, A Data Collection and Graphing Program for the Macintosh IIx using a MacADIOS A/D board.
6. Alspach, D.A., *HEBCAP.c*, A Post-Processing Package for the Macintosh SE for the Conversion of MacADIOS.SZ signals into temperature measurements.
7. Sabadell, A.J., Wenograd, J., and Summerfield, M., "Measurements of Temperature Profiles through Solid-Propellant Flames Using Fine Thermocouples," *AIAA Journal*, Vol. 3, No. 9, pp.1580-1584. (1965)
8. Kubota, N., "Survey of Rocket Propellants and Their Combustion Characteristics", in *Fundamentals of Solid-Propellant Combustion* (Kuo, K., and Summerfield, M.(eds)), AIAA Progress in Aeronautics and Astronautics Series, Volume 90, AIAA, 1984.
9. *Handbook of Chemistry and Physics*, 57<sup>th</sup> Edition, CRC Press
10. Lydensen, A.L., *Fluid Flow and Heat Transfer*, Wiley, New York, (1979), p. 236.
11. Incropera, F.P. and DeWitt, D.P., "Thermophysical Properties of Gases at Atmospheric Pressure", Table A.4, *Fundamentals of Heat Transfer*, Wiley, New York, (1981).
12. Edwards, J.T., *Solid Propellant Flame Spectroscopy*, AFAL-TR-88-076, Air Force Astronautics Lab, Edwards AFB, CA, August 1988.
13. Beckstead. M.W., "A Model for Ammonium Nitrate Composite Propellant Combustion", *26th JANNAF Combustion eeting*, [1989].